Interactions between directly- and parametrically-driven vibration modes in a micromechanical resonator

H. J. R. Westra,[1,*] D. M. Karabacak,[2] S. H. Brongersma,[2] M. Crego-Calama,[2] H. S. J. van der Zant,[1] and W. J. Venstra[1]

[1]*Kavli Institute of Nanoscience, Delft University of Technology, Lorentzweg 1, 2628 CJ Delft, The Netherlands*

[2]*Holst Centre / imec The Netherlands, High Tech Campus 31, 5656 AE Eindhoven, The Netherlands*

(Received 20 July 2011; revised manuscript received 29 September 2011; published 25 October 2011)

The interactions between parametrically- and directly-driven vibration modes of a clamped-clamped beam resonator are studied. An integrated piezoelectric transducer is used for direct and parametric excitation. First, the parametric amplification and oscillation of a single mode are analyzed by the power and phase dependence below and above the threshold for parametric oscillation. Then, the motion of a parametrically-driven mode is detected by the induced change in resonance frequency in another mode of the same resonator. The resonance frequency shift is the result of the nonlinear coupling between the modes by the displacement-induced tension in the beam. These nonlinear modal interactions result in the quadratic relation between the resonance frequency of one mode and the amplitude of another mode. The amplitude of a parametrically-oscillating mode depends on the square root of the pump frequency. Combining these dependencies yields a linear relation between the resonance frequency of the directly-driven mode and the frequency of the parametrically-oscillating mode.

DOI: 10.1103/PhysRevB.84.134305 PACS number(s): 85.85.+j, 05.45.−a, 46.32.+x

I. INTRODUCTION

Parametric amplification and oscillations occur when in a resonant system, one of the system parameters (e.g. spring constant, effective mass) is modulated. The principle is used in low-noise electronic amplifiers[1,2] and to increase the broadband gain in fiber optics.[3–5] In mechanical resonators, parametric oscillations are typically obtained by modulation of the spring constant.[6–9] Applications of parametric resonances in nano- and micro-electromechanics[10] (NEMS and MEMS) include quality(Q)-factor enhancement,[11,12] bit storage, and bit flips using the bistable phase in a parametric oscillator.[13,14] Parametric amplification can also be used for noise squeezing in a coupled qubit-resonator system[15] and was recently observed in carbon nanotube resonators.[16]

Another interesting phenomenon in NEMS is the interaction between different vibration modes. Motivated by the trend toward large scale integration of resonators, researchers study the interactions between several resonators.[17] Recently, nonlinear modal interactions between the flexural modes in a clamped-clamped beam resonator[18–20] and a cantilever[21] have been reported: it has been shown that the resonance frequency of one mode depends quadratically on the amplitude of another mode.

Here, we explore the modal interactions between a directly- and a parametrically-driven mode, yielding a *linear* dependence of the resonance frequency of the directly-driven mode on the pump frequency of the parametrically-driven mode. In Sec. II, the experimental conditions are provided. The following section reports on a detailed analysis of the piezoelectrical parametric amplification of a single mode. Section IV discusses the modal interactions between a directly-driven and a parametrically-pumped mode, and this is the central result of this work.

II. DEVICE DETAILS

The resonators are clamped-clamped beams fabricated from 500 nm thick low-stress silicon nitride (SiN). A stack of platinum, aluminum nitride (AlN), and Pt (100-400-100 nm thick) is sputtered on top to form an integrated piezoelectric transducer (piezo). Figure 1(a) shows a scanning electron micrograph of the device; the white arrow indicates the transducer. The resonators are freely suspended by a through-the-wafer etch. Two lengths are used: $L = 500$ and 750 μm. The width of both resonators is 45 μm. Details of the fabrication procedure are described in Ref. 22. An ac voltage on the piezo produces a force on the resonator and at the same time modulates its spring constant. Both the force and the spring constant depend linearly on the voltage. The voltage on the piezo, V_{out}, is composed of two frequencies, one to directly excite the resonator and one to parametrically pump it, i.e., $V_{\text{out}} = V_{\text{direct}} \cos(\Omega t) + V_{\text{pump}} \cos(2\Omega t + \phi)$, where Ω is the drive frequency and ϕ the phase difference between the two voltages.

The motion of the resonator is measured using an optical deflection setup, as depicted in Fig. 1(b). Frequency spectrum and network analyzer measurements are implemented in a digital signal processor. Measurements are conducted in the vacuum at a pressure of 10^{-4} mbar and at atmospheric pressure. For direct driving, the frequency responses at the first and second modes in the vacuum are shown in Figs. 1(c) and 1(d), with $Q_1 = 6500$ and $Q_2 = 19\,600$.[23]

III. PARAMETRIC AMPLIFICATION OF A SINGLE MODE

The time-dependent part of the equation of motion of the piezoelectric resonator including parametric modulation of the spring constant is described by

$$m\ddot{u} + \frac{m\omega_{\text{R}}}{Q}\dot{u} + \left[m\omega_{\text{R}}^2 + k_p \sin(2\Omega t + \phi)\right]u + \alpha u^3 = F\cos(\Omega t). \quad (1)$$

Here, $u(t)$ is the amplitude of the mode, m is the effective mass, F is the direct drive force, and ω_{R} is the resonance frequency. The dots denote taking the derivative to time. The spring constant is modulated at twice the drive frequency Ω with modulation strength k_p. The α accounts for the Duffing

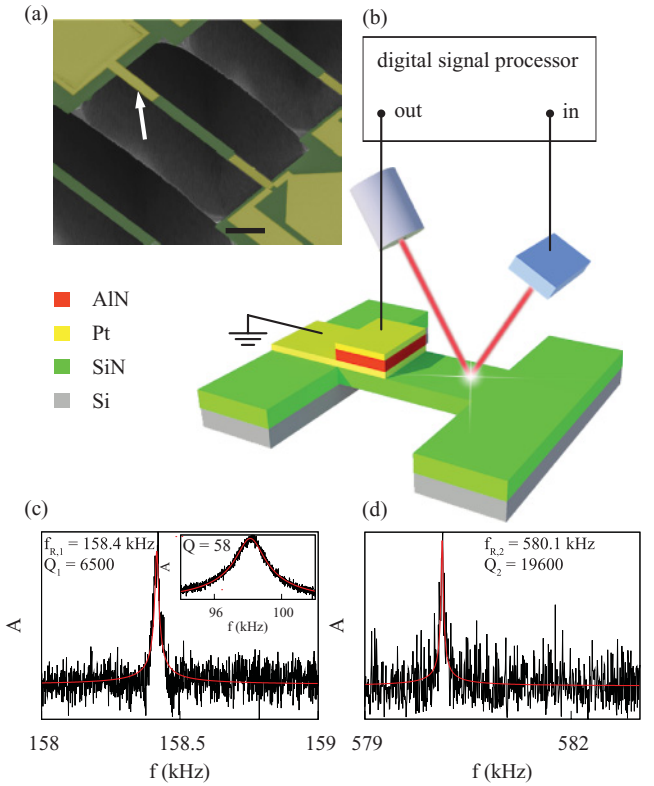

FIG. 1. (Color online) Measurement setup. (a) False-colored scanning electron micrograph of a SiN beam with the piezo actuator (white arrow) on top (scale bar is 20 μm). (b) Optical deflection setup is used to detect motion in air and the vacuum. The piezoactive AlN layer is depicted in red. The piezo actuator and photodiode are connected to a digital signal processor. (c), (d) Typical frequency responses of the first and second modes (amplitude A), respectively, in the vacuum. The inset in (c) shows the frequency response in air, of the resonator with length 750 μm, with a resonance frequency of 98 kHz. The response of a damped-driven harmonic oscillator is fitted through the responses to obtain Q factors and resonance frequencies.

nonlinearity with $\alpha > 0$ for clamped-clamped beams.[24] The parametric gain G is defined by the ratio between the amplitude of the motion with and without parametric drive, and can be calculated from Eq. (1):[25,26]

$$G(\phi) = \sqrt{\frac{\cos^2(\phi/2)}{(1+k_p/k_t)^2} + \frac{\sin^2(\phi/2)}{(1-k_p/k_t)^2}}. \qquad (2)$$

This equation holds for small amplitude vibrations, where the nonlinearity can be neglected. Depending on ϕ, the motion is amplified ($G > 1$) or attenuated ($G < 1$). Above the threshold parametric pump, $k_p > k_t$ with $k_t = 2m\omega_R^2/Q$, the resonator is parametrically oscillating.

Parametric behavior is demonstrated for a resonator with length 750 μm vibrating in air, with $f_{R,1} = 98$ kHz and $Q_1 = 58$ [frequency response in the inset of Fig. 1(c)]. To amplify the motion, the resonator is driven parametrically at $2f_{R,1}$ with $\phi = -0.75\pi$. Figure 2(a) shows the Q factor of the resonator as a function of the parametric pump voltage. The Q factor increases by a factor of 1.7 when the parametric

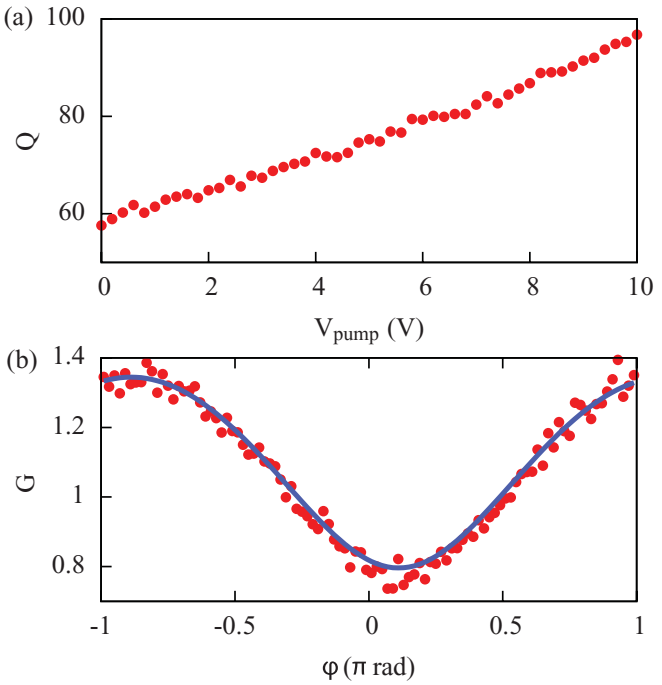

FIG. 2. (Color online) Characterization of the parametric amplification in air. (a) Q-factor enhancement is proportional to the parametric pump voltage. (b) Measured gain vs phase relation; the solid blue line represents Eq. (2), with fit parameter $k_p/k_t = 0.26$.

pump is 10 V. Furthermore, the phase dependence of the gain at 10 V parametric pump is plotted in Fig. 2(b). The gain varies periodically with the phase difference with a period of 2π. The minimum gain is smaller than one, indicating destructive interference by an out-of-phase parametric signal. Equation (2) fits the measured data well with $k_p = 0.26\,k_t$. In these experiments the parametric driving is below the parametric threshold k_t. A further increase of the pump voltage is not possible as this would damage the piezostack. To study parametric oscillation, further experiments are conducted in the vacuum. Here the Q factor improves by two orders of magnitude [Fig. 1(c)], enabling post-threshold driving.

Figure 3 summarizes the measurements of the parametric oscillations performed in the vacuum. A 500 μm long resonator is used, for which the frequency response is plotted in Fig. 1(c). Frequency spectra are measured for three parametric pump voltages in Fig. 3(a). At 80 mV no sign of oscillation is observed (lower panel), and the onset of parametric oscillation is found around 85 mV as shown in the middle panel. A further increase of the pump voltage (upper panel) results in a larger oscillation amplitude. Here, the nonlinear term in Eq. (1) results in an amplitude-dependent resonance frequency. Figure 3(b) shows network analyzer measurements of the resonator amplitude (color scale) as a function of the pump voltage. The resonator is driven directly and parametrically with $\phi = -0.65\pi$. A direct drive signal, weak enough to operate the resonator in the linear regime when $V_{pump} = 0$, is applied to initiate the motion. The motion of the weakly driven resonator is coherently amplified by the parametric excitation, and the amplitude increases with V_{pump}. The

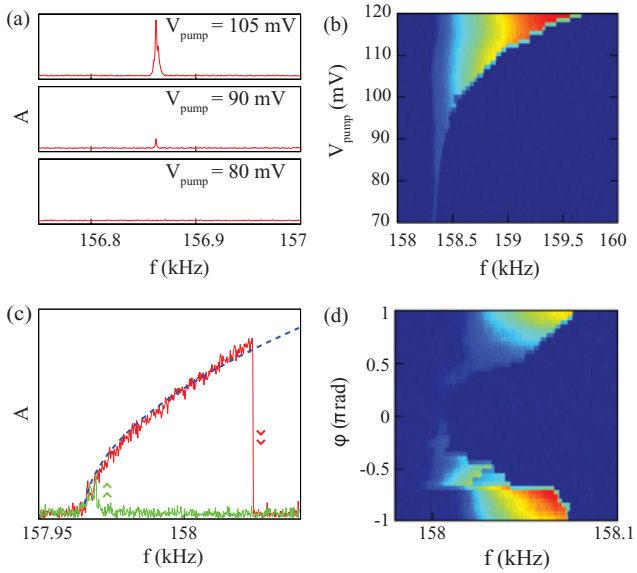

FIG. 3. (Color online) Parametric oscillations of the first flexural mode in the vacuum. (a) Frequency spectra at three pump voltages; the parametric oscillation becomes visible when $V_{\text{pump}} > 85$ mV. (b) Parametric tongue, showing frequency responses when the resonator is driven directly ($V_{\text{direct}} = 5$ mV) and parametrically past the instability threshold. Color indicates the amplitude of oscillation. (c) Hysteresis between the forward (red) and reverse sweep (green) when driving parametrically ($V_{\text{pump}} = 95$ mV). The blue dashed line shows the square root dependence of the amplitude A on the frequency f. (d) Phase dependence of the parametric oscillations at $V_{\text{pump}} = 95$ mV. The color indicates the amplitude of oscillation.

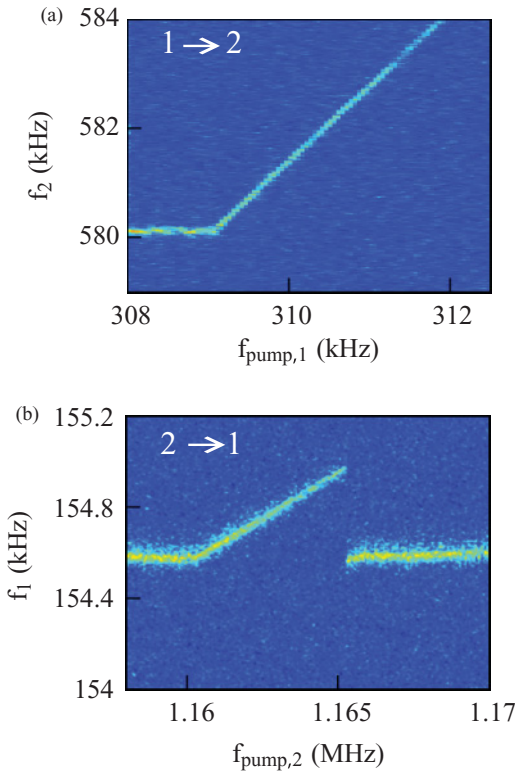

FIG. 4. (Color online) Interactions between a directly- and parametrically-driven mode. (a) Frequency responses of the second mode while varying pump frequency of the first mode. Color scale indicates the amplitude of the second mode. The linear dependence of $f_{\text{R},1}$ on $f_{\text{pump},2}$ is observed as explained in the text. (b) Reversed experiment: frequency responses of the first mode for varying the pump frequency of the second mode.

observed frequency stiffening is expected for a cubic spring constant $\alpha > 0$. The oscillation sustains over a few kHz when the frequency is swept forward. The amplitude shows a hysteretic response when the frequency is swept back [see Fig. 3(c)]. The amplitude of the oscillation depends on the square root of the frequency (dashed blue line).[25] To study the relation between the parametric oscillation amplitude and the phase ϕ, the resonator is parametrically excited above the threshold. Figure 3(d) shows the amplitude of the oscillation when the direct drive frequency is swept while varying the phase difference. Depending on the phase between the direct drive and the parametric excitation, constructive or destructive interference occurs which results in amplification or attenuation of the motion induced by the weak signal that initiates the motion. The maximum parametric amplification is found at a phase difference of $-\pi$ and π. The experiments described above clearly demonstrate the parametric behavior.

IV. COUPLING BETWEEN PARAMETRIC AND DIRECT DRIVEN MODES

We now investigate the interactions between the different vibrational modes of the same mechanical resonator, when one of the modes is parametrically oscillating. This requires us to monitor the response of one mode while another mode is parametrically excited. In particular, the interactions between the first and second modes are considered. First, we study the effect of the parametric oscillations of the first mode, characterized in the previous section, on the resonance frequency of the second mode. Figure 4(a) shows frequency responses of the second mode, when the first mode is parametrically pumped around its resonance frequency. The first mode is only parametrically excited and no direct drive at the resonance frequency is applied. Below the resonance frequency of the first mode, no change in the resonance frequency of the second mode is observed. Pumping at twice the resonance frequency, the first mode starts to oscillate parametrically. This oscillation induces a significant shift in the resonance frequency of the second mode. By parametrically exciting the first mode, the resonance frequency of the second mode is tuned over more than 200 times the resonator linewidth. There is a linear relation of $f_{\text{R},2}$ on $f_{\text{pump},1}$ with sensitivity $f_{\text{R},2}/f_{\text{pump},1} = 1.4$ Hz/Hz.

The change in the resonance frequency is explained as follows: the oscillation of the first mode increases the tension in the beam. This tension tunes the resonance frequency of the second mode to a higher value. A linear dependence between the two frequencies is expected, as in clamped-clamped beams the resonance frequency of one mode depends quadratically on the amplitude of the other mode,[18] i.e., $f_{\text{R},i} \sim |A_j|^2$ for modes i and j. The amplitude of the parametric oscillation depends on the square root of the pump frequency $|A_j| \sim$

$\sqrt{f_{\mathrm{pump,j}}}$,[25] as experimentally verified in Fig. 3(c). Combining these two dependencies, one expects $f_{\mathrm{R},i} \sim f_{\mathrm{pump},j}$. This linear dependence is clearly observed in the measurements [see Fig. 4(a)].

We have also studied the influence of the parametrically-excited second mode on the resonance frequency of the first mode, i.e., the first mode is now probing the second mode, which is parametrically oscillating. Again, a linear dependence of the resonance frequency on the parametric pump frequency is found, as is shown in Fig. 4(b). In this case, the sensitivity $f_{\mathrm{R},1}/f_{\mathrm{pump},2} = 79$ mHz/Hz. As the pump frequency $f_{\mathrm{pump},2}$ is increased above 1.165 MHz the parametric oscillation disappears, and the resonance frequency of the first mode jumps back to its original value. At this point, the nonlinearity causes the oscillation of the second mode to jump to the low amplitude state, which is reflected by the sharp transition of the resonance frequency of the first mode. The large difference in sensitivity with the reversed experiment in Fig. 4(a) indicates that parametric pumping of the second mode is less effective to change the resonance frequency of the first mode than vice versa. This can be understood since the first mode has the largest oscillation amplitude and can provide the largest tension in the beam.

V. CONCLUSION

The interactions between a directly- and a parametrically-oscillating mode of the same mechanical resonator are studied. The parametric amplification and oscillations of a clamped-clamped resonator with an integrated piezoelectric transducer are investigated in detail. The dependence of the oscillation amplitude on pump frequency and phase difference are in agreement with theory. In this work, we demonstrate that the parametric oscillation of one mode induces a change in the resonance frequency of the other vibrational modes. This frequency change is proportional to the pump frequency, as is shown for the first and second modes. The sensitivity of the resonance shift of the second mode on the pump frequency of the first mode is found to be 1.4 Hz/Hz. When the experiment is reversed, i.e., the oscillating second mode is detected by a shift in resonance frequency of the first mode, the sensitivity is 79 mHz/Hz.

ACKNOWLEDGMENTS

The authors acknowledge financial support from the Dutch funding organizations FOM (Program 10, Physics for Technology) and NanoNextNL (Program 6A).

*h.j.r.westra@tudelft.nl

[1] B. Yurke, P. G. Kaminsky, R. E. Miller, E. A. Whittaker, A. D. Smith, A. H. Silver, and R. W. Simon, Phys. Rev. Lett. **60**, 764 (1988).
[2] V. Radeka and R. L. Chase, IEEE Trans. Nucl. Sci. **13**, 477 (1966).
[3] Y. Zhang, H. Wang, X. Li, J. Jing, C. Xie, and K. Peng, Phys. Rev. A **62**, 023813 (2000).
[4] M. E. Marhic, N. Kagi, T. K. Chiang, and L. G. Kazovsky, Opt. Lett. **21**, 573 (1996).
[5] A. A. Savchenkov, A. B. Matsko, M. Mohageg, D. V. Strekalov, and L. Maleki, Opt. Lett. **32**, 157 (2007).
[6] R. Lifshitz and M. C. Cross, Phys. Rev. B **67**, 134302 (2003).
[7] R. B. Karabalin, R. Lifshitz, M. C. Cross, M. H. Matheny, S. C. Masmanidis, and M. L. Roukes, Phys. Rev. Lett. **106**, 094102 (2011).
[8] K. L. Turner, S. A. Miller, P. G. Hartwell, N. C. MacDonald, S. H. Strogatz, and S. G. Adams, Nature (London) **396**, 149 (1998).
[9] M. Zalalutdinov, K. L. Aubin, M. Pandey, A. T. Zehnder, R. H. Rand, H. G. Craighead, and J. M. Parpia, Appl. Phys. Lett. **83**, 3281 (2003).
[10] K. L. Ekinci and M. L. Roukes, Rev. Sci. Instrum. **76**, 061101 (2005).
[11] I. Mahboob and H. Yamaguchi, Appl. Phys. Lett. **92**, 253109 (2008).
[12] J. Tamayo, J. Appl. Phys. **97**, 044903 (2005).
[13] I. Mahboob and H. Yamaguchi, Nat. Nanotechnol. **3**, 275 (2008).
[14] I. Mahboob, E. Flurin, K. Nishiguchi, A. Fujiwara, and H. Yamaguchi, Nat. Commun. **2**, 198 (2011).
[15] J. Suh, M. D. LaHaye, P. M. Echternach, K. C. Schwab, and M. L. Roukes, Nano Lett. **10**, 3990 (2010).
[16] A. Eichler, J. Chaste, J. Moser, and A. Bachtold, Nano Lett. **7**, 2699 (2011).
[17] R. B. Karabalin, M. C. Cross, and M. L. Roukes, Phys. Rev. B **79**, 165309 (2009).
[18] H. J. R. Westra, M. Poot, H. S. J. van der Zant, and W. J. Venstra, Phys. Rev. Lett. **105**, 117205 (2010).
[19] T. Dunn, J.-S. Wenzler, and P. Mohanty, Appl. Phys. Lett. **97**, 123109 (2010).
[20] I. Mahboob, Q. Wilmart, K. Nishiguchi, A. Fujiwara, and H. Yamaguchi, Phys. Rev. B **84**, 113411 (2011).
[21] W. J. Venstra, H. J. R. Westra, and H. S. J. van der Zant, Appl. Phys. Lett. **99**, 151904 (2011).
[22] D. M. Karabacak, S. H. Brongersma, and M. Crego-Calama, Lab Chip **10**, 1976 (2010).
[23] During the experiments, the drift of the resonance frequency is within 3% .
[24] W. Zhang, R. Baskaran, and K. L. Turner, Sensors and Actuators A **102**, 139 (2002).
[25] R. Lifshitz and M. C. Cross, *Nonlinear Dynamics of Nanomechanical and Micromechanical Resonators*, Vol. 1 (Wiley, Meinheim, 2008), Chap. 1, pp. 1–52.
[26] D. Rugar and P. Grütter, Phys. Rev. Lett. **67**, 699 (1991).